A Measurement-informed Approach to Modeling Underground IoT Communications

Rummana Rahman*, Cheng-Hsun Lin†, Cheng-Hsin Hsu†, and Nalini Venkatasubramanian*
*Department of Computer Science, University of California, Irvine, {rummanar, nalini}@uci.edu
†Department of Computer Science, National Tsing Hua University, chlin147@gapp.nthu.edu.tw, chsu@cs.nthu.edu.tw

2024 IEEE 100th Vehicular Technology Conference (VTC2024-Fall) | 979-8-3315-1778-6/24/$31.00 ©2024 IEEE | DOI: 10.1109/VTC2024-Fall63153.2024.10757716

***Abstract*—Smart city transportation infrastructure will soon demand the development of reliable underground IoT (IoUT) communication. In this paper, we develop a novel analytical model, MAME (Material Aware Measurement Enhanced), to capture signal propagation properties in wireless IoUT networks to achieve reliable data transport. A driving motivation is monitoring underground infrastructure systems (e.g., pipelines and storm drains) for early detection of anomalies and failures to guide human investigation and intervention. We analyze the feasibility of successfully receiving wireless data packets from underground (UG) sensor nodes through multiple material layers and under diverse environmental conditions. Our proposed approach integrates physics-based modeling and empirical studies with small-scale testbeds (in our lab and outdoors) with multiple channel setups and physical layer attributes. We derive a novel MAME approach to model signal propagation in both 802.11-based WiFi and LoRaWAN networks. The resulting MAME model is shown to capture communication behavior in WiFi and LoRaWAN networks accurately. The MAME model is used to augment the popular NS3 simulator to explore scaled-up underground networks and varying channel conditions (e.g., soil moisture level). Such a combined analytical-empirical approach will enable the communication control plane and application layer to better predict channel conditions for improved IoUT network design.**

***Index Terms*—Underground infrastructures, wireless sensor network, reliable communication**

I. Introduction

The rise in urban populations have created a need for better management of buried assets and critical infrastructure, e.g., water and gas pipelines, optical fiber trunks, stormwater systems, and more. These underground systems are aging and fragile, causing resilience concerns, and increase the need for real-time monitoring to ensure infrastructure health and rapidly detect undesirable events (e.g., damaged lines, water leaks, pollutant flows). Decision support for maintenance and time-critical alerts requires adequate instrumentation of sensing infrastructure that can obtain and communicate data from geo-distributed locations to servers for analyses [1].

Infrastructure resilience for roads and highways is critical for maintaining flawless transportation, especially in case of emergency situations, i.e., natural disasters. The understanding of the underground infrastructure status can add to road safety, commuting reliability, damage prevention of the structures, and early prediction of congestion from elevated-risk areas. Consider municipal stormwater networks that transport rainwater and nuisance flows (e.g., excess irrigation) from cities to receiving waters (e.g., rivers, bays, ocean). These systems are comprised of numerous physical components distributed regionally (in catchment areas). Urban activities, such as commercial, household, and industrial processes, yield a variety of harmful pollutants (pesticides, oils, and greases) and create water-quality problems [2]. Current approaches are time-consuming and ineffective: monitoring consists of citizen reports, manual site visits, and human grab sampling [2]–[4]. The availability of low-cost and low-power sensor devices for monitoring physical phenomena (such as fluid flow, pressure, temperature, etc.) is creating the possibility of obtaining information in near real-time. However, communicating this data in time for analysis remains challenging.

A key issue in Underground IoT (IoUT) systems is the lack of reliable wireless communication [5] infrastructure in underground environments that consists of heterogeneous materials including soil, concrete, metal, water, air, etc. [6]. Today, reliable data transport for underground communications largely relies on expensive, hard-to-deploy, and error-prone wired networks, which are more vulnerable to network outages during renovation and maintenance. Existing efforts in wireless sensors for smart agriculture that involve low-depth sensor deployments in a single medium (soil) or customized deployments with non-traditional radios (in §II) are unsuitable for deployments at scale in infrastructure networks. What is missing at a fundamental level is a comprehensive approach to model IoUT communications and channel characteristics, especially in complex real-world infrastructure settings.

In this paper, we tackle the limitations of the existing channel models that fail to capture complex underground communications properly. Multiple varied propagation characteristics based on medium-specific and exogenous factors, such as the type of soil, moisture level of soil, and type of concrete, topographical features, and weather-related conditions, including evapo-transpiration factors, play a role. We develop a modeling methodology that couples a physics-informed empirical approach through focused measurement studies in the target deployment setting. Particularly, we present the Material-Aware Measurement-Enhanced (MAME) approach, which allows infrastructure providers to adopt a design mindset that would accommodate system-level sensing and monitoring. It allows for lower-cost retrofits for aging systems to help monitor unexpected conditions and service degradation. To the best of our knowledge, the MAME methodology is the first of its kind to help model and instrument the next generation of smart underground community infrastructures.

Contributions of this paper. We develop a Material-Aware

Measurement-Informed channel modeling approach for IoUT that can be adapted to different material layers, while their properties and deployment factors can be found in typical infrastructure settings. We make the following contributions:

- We present a generalized framework for IoUT communications and discuss the limitations of existing underground sensing efforts and communication technologies (§II).
- To obtain a quantitative understanding of IoUT, we develop indoor in-lab and outdoor testbeds using off-the-shelf hardware and communication components and conduct multiple measurement studies focused on communication quality (§III).
- We derive theoretical communication models that are Material-Aware (MA model), starting from classical analytical models used for air-based above-ground communications. We enhance the MA model to create the MAME (Material-Aware Measurement-Enhanced) channel models to capture deployment and access features for wireless (LoRa, WiFi) networks (§IV).
- We integrate our proposed channel models in the well-known packet-level simulator NS-3 to enable larger-scale evaluations of emerging IoT sensor networks (§V).

II. MAME: An Integrated Material and Measurement Aware Approach

Studies have pointed to communication reliability issues in underground IoT infrastructures such as water pipelines [7]–[9]–multiple wireless communication methods based on electromagnetic, acoustic, and magneto-inductive wave-based signals report unreliable data transport. Small-scale and customized physical layer measurements [10] to capture RSSI and Packet Drop Rates) have explored small Tx-Rx distances under 1 m. Recent studies with custom low-frequency radio (50-200MHz) [11], [12], have explored the design of path loss models in soil [11], [13], under varying soil conditions. Conceptual frameworks, e.g., [14], that map IoT building blocks with protocols must be extended to capture long-range low-power transmission through highly attenuating channels.

With the arrival of new longer wavelength modules, such as LoRa, LoRaWAN, and LPWAN, with new modulation techniques [15], the possibility of underground signal transfer has seen new opportunities. Recent efforts in smart agriculture [16] have shown that LoRa signals possess a remarkable immunity to multipath fading and interference and hence can propagate longer distances ($>$ 50m) in Under Ground/Above Ground (UG/AG) settings with satisfactory signal strength for shallow soil depth (15 cm). Experiments in diverse soil settings indicate that transmission and environmental parameters (e.g., frequency and spreading factors, moisture level) can significantly impact communication quality.

In contrast to the above efforts, our work on IoUT for built infrastructure (storm drains, pipeline networks) aims to use off-the-shelf radio technologies and IoT communication protocols available, such as LoRa/WiFi, to handle complex layering of materials (concrete, varying types of soil) through which signals must propagate in such deployments. We argue that a comprehensive framework for UG/AG WSN

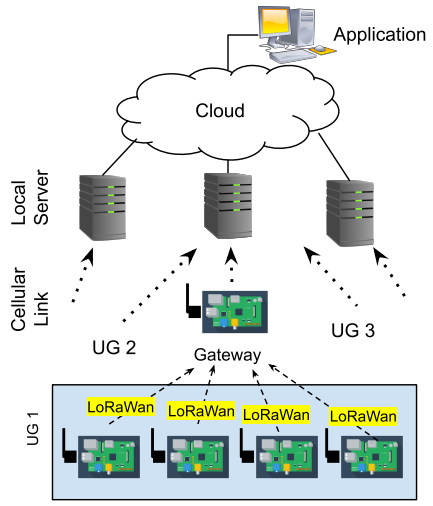

Fig. 1. Our proposed IoUT sensor network consists of end-nodes, gateways, edge servers, cloud servers, and applications.

for infrastructure monitoring would require the design of reconfigurable channel models that consider multiple material layers and a variety of environmental factors. Key challenges in developing such models include the lack of feasible off-the-shelf modules for UG/AG test beds that can accommodate varying carrier wavelengths. A better understanding of signal propagation for varying bandwidths through soils is also required. Finally, a lack of tools to effectively conduct real-time measurement, packet level monitoring, and computation in challenged settings with high error rates makes it difficult to assess the feasibility of wireless deployments in UG/AG systems. Changing environmental factors such as weather, RF interference, and obstacles (large structures, moving vehicles) result in varying signal strengths. Designing a network control plane requires intelligent methods that frequently learn about multiple communication attributes and adjust the network state information for the end nodes accordingly.

To address the above challenges, we propose an integrated model for wireless communication for subsurface nodes buried inside the underground infrastructures, which combines the physical properties of the material layers with empirical measurement studies that capture the deployment setting. We begin by establishing a quantitative model for communication properties, e.g., signal attenuation, through multilayer channels comprising different infrastructure materials. We leverage infrastructure manuals and literature on soil and concrete properties, antenna theory references, and in-person site survey-based data as building blocks toward a conceptual IoUT communication model and network architecture.

Physical Site Surveys. Through a series of in-person site visits to storm drain sites facilitated by municipal public works agencies, we were able to understand the settings and limitations to network feasibility for the existing infrastructures. Initial measurement studies and data pointed to the unreliability of wireless signal transport–signal strengths of conventional mobile LTE networks within the interior of storm drains were found weak and unstable at most critical monitoring locations

instrumented in the storm drain network for insights into the soil depth (few meters) to concrete pipe thicknesses (around 1 foot). As our driving use case, we consider networks of devices 6–16 ft beneath the ground surface with a concrete slab thickness of 6–12 inches. Additionally, we consider a fixed attenuation due to the concrete slab and a variable attenuation of the signal while passing through the soil. This path loss in the soil will depend primarily on the distance between the end node and the gateway. Soil material properties and moisture conditions will also influence the attenuation.

We envision a hierarchical system architecture that considers geospatially distributed leaf sensor nodes at critical locations of the underground stromdrain network. As illustrated in Fig. 1, the sensed data are sent wirelessly to the data collection points placed above-ground, i.e., the gateway (GW) nodes. TCP/IP networks (wireless or wired) communicate with a local server and/or the cloud.

This paper studies the feasibility of IoUT communication by studying signal propagation behavior at the lowest layer of the network, i.e., the physical layer comprising soil and concrete as channel materials. This work considers studies in three phases–1) acquiring the necessary data about materials and their physical properties and performing empirical studies and measurements on multiple small-scale testbeds (controlled lab-based setting, public outdoor deployments), 2) deriving a Material-Aware Measurement-Enhanced (MAME) model combining existing communication theory modeling methods with empirically-obtained measurements, and 3) performing simulation-based studies to observe the effect of the measurement-enhanced model for a scaled-up network. Our work focuses on observable attributes from the off-the-shelf hardware, including the received signal strength index (RSSI) and average throughput in the channel.

III. Measurements in Real Testbeds

Small-scale real-world testbeds were constructed in lab setup for measuring two metrics for adhoc WiFi- i) RSSI and ii) Throughput, as shown in Fig. 6. Experiments were designed to observe the received signal strength and throughput after passing through soil and concrete. A second testbed, shown in Fig. 3, was built outdoors to measure RSSI for LoRaWAN. Both testbeds are used to understand the signal propagation behavior with varying distances. For throughput measurement, only the in-lab set-up was used with a fixed distance. The purpose of these experiments is to apply the findings towards building up a model for larger real-world setups.

Testbed-RSSI-WiFi: The first in-lab setup (Fig. 2a) was constructed on a test bench, with the channel structure laid down in a horizontal alignment to mimic real-world UG to AG channels. The UG channel environment was created using a plastic box-enclosed channel filled with three kinds of soil–sand, silt, and garden soil. Concrete bricks were added at one end of the channel. The sender and receiver nodes were set at the two ends of the channel. The whole setup was covered with multiple layers of aluminum foils to create an isolated environment from the surrounding wireless signals

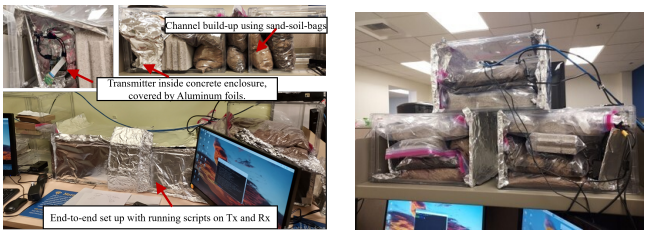

(a) Testbed-RSSI-WiFi (b) Testbed-Throughput-WiFi

Fig. 2. In lab setup constructing channel with WiFi (2.4 GHz).

Fig. 3. Outdoor testbed setup using LoRa (915 MHz).

and to prevent test signal leakage inside the channel. For the hardware, micro-computer modules Raspberry Pi-4 (RPi-4) were used with in-built WiFi modules working at the 2.4 GHz frequency, operating in the ad-hoc WiFi mode, to ensure packet exchange only inside the testing adhoc network.

The RSSI measurements were taken for four different distances, with 200+ measurements for each distance (keeping a concrete-to-soil layer thickness ratio 0.2). These concrete thickness values (2-8 inches) were selected based on stormdrain component manuals (the charts for vertical live load tables of conduit, earth load, pressure distribution, and pipe dimensions) [17]–[19]. This is shown in Table I.

TABLE I
Measured RSSI and Loss with Varying Distances: WiFi

Reading Average for 2.4 GHz from 200 Readings: TxP = 31 dBm		
Soil/Conc. Distance (m)	RSSI (dBm)	Avg-Loss 2-medium
0.46 / 0.05	-40.50 ± 1.67	71.50
0.61 / 0.10	-43.12 ± 2.94	74.12
0.91 / 0.15	-45.64 ± 2.60	76.64
1.22 / 0.20	-45.15 ± 1.68	76.15

Testbed-Throughput-WiFi: The second in-lab set-up (Fig. 2b) was designed to measure throughput using the WiFi module (2.4 GHz). The channel had a 1.5 ft soil layer and 4 inches of concrete bricks. The average throughput was obtained from multiple measurements for a 3-node adhoc WiFi network, where one AG node (running the server) located at the top of the stack received packets from the two UG client nodes. In this approach, among multiple readings, the minimum throughput values were considered, as in the lab environment, partial leakage of the signal through the insulating layers (aluminum foils) was possible. Table II presents the results.

TABLE II
MEASURED THROUGHPUT FOR 3-NODE AD-HOC WIFI NETWORK - (SOIL+CONCRETE MEDIUM AS COMPARED WITH AIR)

AVG Throughput for 2.4 GHz from Multiple Readings: TxP = 31 dBm			
Distance (m)	Client-1	Client-2	Server
soil+concrete(Mbps)	9.60	10.60	9.61, 16.70
air (Mbps)	53.60	56.20	57.80

Testbed-RSSI-LoRa: The outdoor testbed was constructed in a sandpit using LoRaWAN modules, as shown in Fig. 3. The selected frequency band was 915 MHz, and the communication mode was set to LoRaWAN to measure the end node to gateway (GW) signal strength.

For the hardware, two RPi-3 (Model B) were used- one working as the IoUT end node and the other as the GW. The end node (sender) was attached to a Multitech xDot LoRaWAN antenna board via a USB 2.0 port used as a LoRaWAN interface. This xDot module transmitted packets at the US 915MHz frequency band. The other RPi-3, working as the GW, was attached with a RAKwireless RAK2245 Pi HAT WisLink LPWAN Concentrator. This gateway collected packets from the xDot module and forwarded the information to the server. The IoUT node with the xDot module is connected to the laptop via a USB to Transistor-Transistor Logic (TTL) cable. The gateway was connected to the laptop using SSH. The GW is connected to a local WLAN.

As for the software tools setup for this experiment, The Things Network (TTN) was adopted as the server platform. Minicom (a serial communication program that connects to devices through serial ports) was used for AT commands (in the CLI terminal to control the xDot) to read the RSSI values of the received signals. Table III shows the measurement log for RSSI of this LoRa testbed. The RSSI measurements were taken for two setups- a) adding two 4-inch wide (2 inch thick at center) concrete bricks between two IoT devices and b) without the bricks. Measurements were taken for increasing distances in the sand for both setups.

TABLE III
MEASURED RSSI AND LOSS WITH VARYING DISTANCES: LORAWAN

Reading Average for 915 MHz from Multiple Distances: TxP = 30 dBm				
Dist. (m)	RSSI (dBm) (with bricks)	Avg Loss 2-medium (with bricks)	RSSI (dBm) (without bricks)	Avg Loss 2-medium (without bricks)
0.4	-42.00 $\pm$ 1.41	72.00	-52.00 $\pm$ 2.00	82.00
0.8	-48.33 $\pm$ 0.47	78.33	-49.00 $\pm$ 1.00	79.00
1.0	-52.33 $\pm$ 1.25	82.33	-59.00 $\pm$ 0.58	89.00
1.6	-78.33 $\pm$ 0.47	108.33	-67.67 $\pm$ 1.15	97.67
2.0	-95.00 $\pm$ 2.83	125.00	-80.67 $\pm$ 0.58	110.67
2.5	-91.67 $\pm$ 0.47	121.67	-81.00 $\pm$ 0.58	111.00
3.0	-84.00 $\pm$ 0.82	114.00	-84.00 $\pm$ 1.00	114.00

The general noise floor level for LoRa is considered to be -90 dBm. Still, LoRa receivers can demodulate received signals of -7.5 dB to -20 dB below the noise floor, which means an average RSSI of -100 dB or even up to -129 dB can be accepted for a system. This experiment's SNR (Signal-to-Noise Ratio) readings stayed within the window of +7 to +10 dB, which is satisfactorily above the minimum SNR requirement. Hence, we can predict that a little bit farther distance extension of the network would be possible in real-world deployment, which couldn't be deployed within the scope of this study due to resource limitations.

IV. MODELING IOUT COMMUNICATIONS

A. Channel Modelling:

The channel modeling study started with the physics-based intuition that the channel attenuation coefficients would be specific for a specific site, and the model would maintain equivalence among similar kinds of infrastructures. For composite medium, like a combination of concrete and soil in two layers, the existing model based only on soil and shallow depth [11], [13] doesn't fit. This model also depends on figuring out the attenuation coefficients based on the detailed soil grain properties and mineral composite details of the site in consideration, which method is generally not feasible for infrastructure-based channels. Even with that knowledge, the predictions can deviate significantly from the actual measurements due to the soil proportion variations among sites. Hence, our modeling adopted an infrastructure-based approach.

This study started from the antenna theory [20]–[22], for element level analysis using **Friis propagation model** (for homogeneous medium) and took far-field signal propagation into account. The Friis model for air is written as:

$$\begin{aligned} P_{Rx}(dB) =& P_{Tx}(dB) + G_t(dBi) + G_r(dBi) + \\ & 20log(\lambda/(4\pi d)) - 10log(L). \end{aligned} \tag{1}$$

Here, λ is the wavelength. We assume both antenna gains are 1, i.e., $G_t(dBi)$=$G_r(dBi)$=0, and system loss as zero (L=1), which brings in an approximated model for air. The model enhancement, to make it compatible with the non-air mediums, starts by ingesting soil's electric permittivity (ϵ) and magnetic permeability (μ) properties inside the basic Friis model's wavelength factor (or light speed factor), which is shown in the following equation, in terms of transmission frequency, f:

$$\begin{aligned} P_{Rx}(dB) =& P_{Tx}(dB) + 20log(C_o/4\pi) \\ & - 20log(fd) - 10log(\epsilon_r \mu_r). \end{aligned} \tag{2}$$

Note that the attenuation will vary based on the last two terms of the above equation for a specific channel structure with a specific node topology. For an inhomogeneous medium, effective dielectric constant and effective magnetic susceptibility are counted for the overall medium. Hence our preliminary loss model ($Loss = P_{Tx} - P_{Rx} = \Sigma Loss_{medium}$), is the **Material Aware (MA) model**:

$$\begin{aligned} Loss(dB) =& 20log(4\pi/C_o) + 20log(fd) + \\ & 10log(\epsilon_{r_{(eff)}} \mu_{r_{(eff)}}). \end{aligned} \tag{3}$$

To observe the preliminary RSSI pattern with the MA model, applied for an example real-life UG channel, we plotted Fig. 4 with two boundary-frequencies commonly used in the regular infrastructure networks (WiFi and LoRa). Here, the lower-bound-frequency = 433 MHz, upper-bound-frequency = 5.15 GHz, the concrete layer thickness = 1 ft, and the soil-channel distance range is 5 m to 20 m. As a reference,

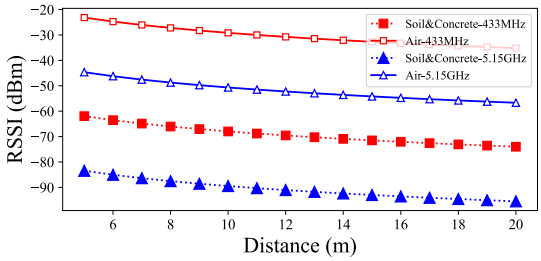

Fig. 4. MA Model for RSSI (dBm) with distance (m) for (Soil+Concrete) channel as compared with Air, for lower bound & upper bound carrier frequencies: 433MHz & 5.15 GHz.

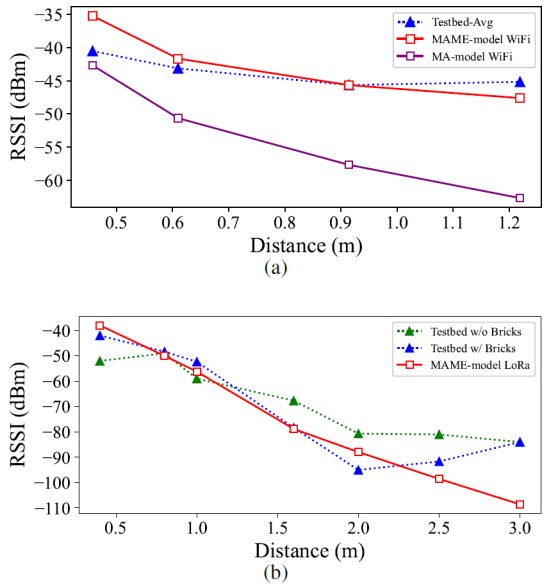

Fig. 5. MAME Model development for RSSI (dBm) with distance (m) for (Soil+Concrete) channel- (a) WiFi: comparing Testbed values, MA-model, and MAME Model (2.4 GHz), (b) LoRa: comparing Testbed values for with brick, without brick, and MAME Model with brick (5.15 MHz).

air-propagation models from the basic Friis models are also plotted for these two frequencies.

The findings from the MA-model show that the RSSI stays above -100 dBm even beyond the transmitter and receiver distance of 15 m. This finding points to the possibility of successful data reception and at the same time encourages further investigation considering the naiveness of this model. Here soil parameter values were picked from a mid-window range from a wide spectrum of values of soil properties [23]–[26] as: $\epsilon^s_{r_{(eff)}}$=23.086 (from complex ϵ^s_r=23 + 2j) and $\mu^s_{r_{(eff)}}$=1 (from complex μ^s_r=1 + 0.0005j). Similarly, for concrete: $\epsilon^c_{r_{(eff)}}$=11.16 (from 10.75+3j) and $\mu^c_{r_{(eff)}}$=1 (from 1+0.00015j) selecting from a wide range of possible values [27]–[29]. An important note here is that all these four parameters, especially the ϵ^c_r and μ^s_r values, are heavily influenced by the chemical composition, moisture levels, minerals/metal percentage in the soil and concrete, and chemical events taking place inside the channel. Hence, these factors can lead to any deviation from the model in the real-life reading. Site-specific measurements can help us to fine-tune the models to higher-accuracy models.

Material Aware-Measurement Enhanced Model-WiFi: The preliminary MA model is tuned with our WiFi-testbed parameters (with f and varying d) and compared with the ground truth values (see Fig. 5a). A considerable gap with a linear shift of the model from the ground truth (with increasing distance) suggests some necessary corrections. Hence, the naive MA model gets modified to the **Material Aware Measurement-Enhanced-model (MAME)**, for the WiFi network, by adding a linear correction term, i.e., αd. The MAME model is written as:

$$Loss(MAME)_{wifi} = 20log(4\pi/C_o) + 20log(fd) + 10log(\epsilon_{r_{(eff)}}\mu_{r_{(eff)}}) - \alpha d. \quad (4)$$

The best-fit coefficient value is: $\alpha = 10$ for our **MAME-WiFi** model (with a concrete-to-soil-thickness ratio of 0.2).

Material Aware-Measurement Enhanced Model-LoRa: Progressing further from the MAME-WiFi model, an extended model suitable for LoRaWAN was studied in our final modeling work. This LoRa-based model considered a fixed-depth concrete layer (of 2") and varying soil distance matching with the parameter values of the LoRa-Testbed. In this model **(MAME-LoRa)**, $\epsilon^s_{r_{(eff)}}$ value was changed to sand-type soil's permittivity.

From close investigation, some important findings were established for this model: a) far-field ($d > 3\lambda$) RSSI pattern differed from the near-field (approx. 1 m, for 915 MHz), b) even inside the near-field region, the reactive and the radiative fields can differ noticeably due to the channel properties of soil or concrete. Hence, MAME-LoRa model considers distance-based coefficient values for different ranges, where α=8 for $d_{concrete}$=2", 6 for d_{soil}<1m, 15 for d_{soil}>1m. In particular, we write the MAME-LoRa model as:

$$Loss(MAME)_{lora} = 20log(4\pi) + 32log(d) + \beta log(1/\lambda_{med}) + \alpha d. \quad (5)$$

Here, the values of β, λ_{med}, and α are signatory for a specific channel structure combined with its material properties. For MAME-Friis-LoRa model, regarding the outdoor testbed: $\beta_{concrete}$=20 , β_{soil}=32, and λ_{med}=$C_o/f\sqrt{\epsilon_{r_{(eff)}}\mu_{r_{(eff)}}}$; and $\epsilon^s_{r_{(eff)}}$=31, $\epsilon^c_{r_{(eff)}}$=11.9, and $\mu^s_{r_{(eff)}}$ = $\mu^c_{r_{(eff)}}$ = 1.

Last, we combine Eqs. (4) and (5) into the following general-MAME-Friis model:

$$Loss(MAME)_{general} = 20log(4\pi) + \gamma log(d) + \beta log(1/\lambda_{med}) \pm \alpha d, \quad (6)$$

where the coefficients, γ, β, and $\pm\alpha$ are infrastructure-specific and will stay within a range of values based on the network. Hence, these coefficients can be learned for infrastructures from real-life data. In all these three plots from the two testbeds, we find knee-points at the junction of near and far fields. With the LoRa-with-brick setup, the ground truth reading behaves differently than the theoretically expected pattern. The reason could be that, for that distance, a secondary wavelet that early escapes to air, precedes the primary wavelet with less propagation delay and a higher RSSI. The same reason might be causing the RSSI to go up at a 2 m distance.

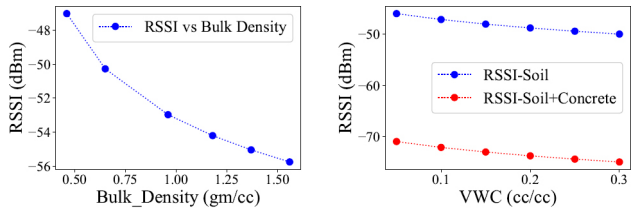

(a) RSSI vs Bulk Density (b) RSSI vs VWC

Fig. 6. MA-model depicting influence of Bulk Density and VWC on RxPower for a soil distance=30.27m and carrier frequency of 433 MHz: (a) Varying bulk density for a fixed VWC of 5% and (b) Varying VWC for a fixed bulk density of 0.96 gm/cc.

Additional tuning knobs, some considered in the next analysis, include the environmental factors and material properties that can influence the signal attenuation, such as soil moisture, soil particle diameter, sand/clay ratio, and soil density.

B. Environmental Factors:

In our 2nd phase of modelling, we analyzed the effect of varying soil properties and environment on the signal strength. Soil physics consists of varying range of soil types and moisture levels. For simplification purposes, soil granularity and its sand-clay portion property can be integrated into one parameter– bulk density. With further simplification and approximations, this bulk density and the soil's moisture status, i.e., soil volumetric water content (VWC), can be integrated into a single medium property, the refractive index of the soil [30]. We chose the simplest bivariate model for the refractive index: $Ref\_index = (9.93 \times vwc) + (2.454 \times b\_density) - 1.208$.

Figs. 6a and 6b show our analysis on the effect of the soil density and moisture as we ingested this bivariate model into our MA-model for 433 MHz carrier frequency, with a fixed Tx-Rx distance of 30.27 m. For the soil density analysis, in Fig. 6a, we skipped modelling for the concrete considering that the concrete layer in this case will stay with a fixed loss (an additional 25 to 35 dBm for the thickness range of 2" to 10"). We modelled the medium as soil-only and varied the bulk density from 0.46 gm/cc to 1.56 gm/cc, keeping the moisture level constant (VWC=5%). After the loss in the soil channel the RSSI level was found above -60 dBm, which would result in a final RSSI of approx -95 dBm, when combined with loss in concrete, at the receiving end.

For analyzing the effect of the water content level on the received signal strength (shown in Fig. 6b), the communication parameters (distance and frequency) were kept the same and the VWC was varied from 5% to 30% keeping the soil's bulk density fixed at 0.96 gm/cc. The impact of VWC on RSSI is found to be significant as RSSI drops significantly from -45 dB to -50 dB, for a soil-only channel, with the increasing VWC. With an additional layer of concrete, adding a loss of 25 dB, the RSSI lowest point stays around -75 dB.

V. Simulation Studies with MAME

We next study the feasibility of wireless data reception from IoT nodes situated at farther distances in a real-life setting. We used the industry-standard network simulator NS3 to simulate the MAME models for scaled-up networks (WiFi and LoRa). NS3 is designed for conventional wireless communication through air. The physical layer libraries (propagation-loss-model) of NS3 were modified with the material properties of concrete and soil, with the permittivity values derived from the MAME model. The average bulk density was taken as 2.74 gm/cc and the VWC as 0.5%. A concrete thickness of 5 inches, with a fixed loss, was considered.

Experiments were run with three network topologies–1) point-to-point, 2) 1 Access Point & 5 end-nodes (for WiFi), and 3) 2 GW & 10 end-nodes (for LoRa). The senders were situated at different coordinate points so the Tx-Rx distance gets a varying range. Keeping the use case in mind, low data rates were considered. The simulation setup parameters for WiFi and LoRa are elaborated in Table IV.

TABLE IV
NS3 Simulation Setup Parameters

WiFi 2.4 GHz and LoRa 868 MHz		
Parameters	WiFi (TxP 16dB)	LoRa (TxP 14dB)
Topology	1 AP-5 ED	2 GW- 10 ED
Model	MAME-WiFi	MAME-LoRa
Packet size	1024 Bytes	19 Bytes
Packet interval	0.05-0.15 sec	1-5 sec
Channel length	0m-1.5m, 0m-3.1m	0-3m, 0-6m
Channel VWC	N/A	0.05% to 30%

The result of a number of simulation experiments is summarized in Fig. 7. In the physical layer metric measurement, RSSI (in Figs. 7a and 7b), the output varied in a range of -49.0 to -60.4 dBm for WiFi and within -68 to -177 dBm for LoRa. These results closely followed the MAME model.

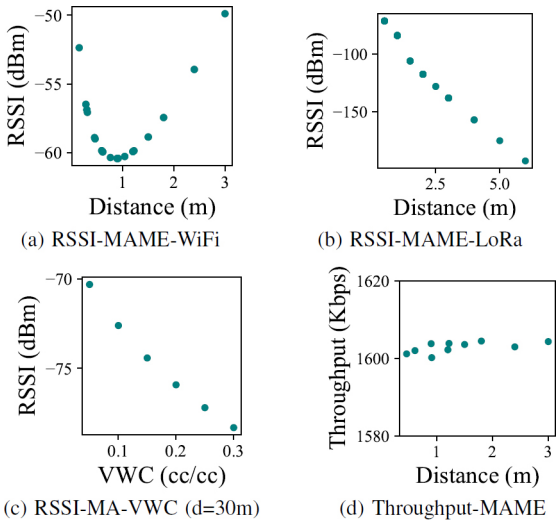

(a) RSSI-MAME-WiFi (b) RSSI-MAME-LoRa
(c) RSSI-MA-VWC (d=30m) (d) Throughput-MAME

Fig. 7. NS3 simulation results: (a), (b)- RSSI implementing MAME model, (c) RSSI- using MA model, (d) WiFi-Throughput using MAME model.

However, there is an upper bound in distance (2m for WiFi, 3m for LoRa), after which real-life data might deviate from the model. One reason is that the MAME model considered secondary wavelet propagation of the signal, which is distance-specific. For LoRa, the upper bound will be set at

a distance from where signal strength becomes unusable for demodulation below -120 dB. In our simulation, the LoRa MAC layer module dropped 50% of the packets arriving from nodes farther than 3m (below -129 dB). By setting the TxP at a higher power level, a longer distance range can be achieved.

The next simulation experiment, shown in Fig. 7c measured RSSI with varying VWC, using MA-model only (as we do not have any testbed-based model for VWC yet), for 868 MHz, soil-only channel, and a fixed Tx-Rx distance of 30.27 m, in NS3. This simulation result shows much optimistic values of RSSI, as we implemented the naive MA model in this simulation experiment, as no testbed-measurement based derived model is there yet.

Lastly, we studied throughput for WiFi networks (2.4 GHz) in NS3, for a channel of 4 inches concrete and soil thickness varying from 0m to 3.1m (Fig. 7d). The throughput for the AP node was 1.603 Mbps (AVG). Although our in-lab testbed throughput was 9.61 Mbps (AVG), it is acceptable, as our RPi modules ran commands with a higher number of packets per second and in some cases detected the maximum possible throughput. We also predict that any secondary wavelet signals leaked through the insulated walls might have also contributed to this higher throughput in the real-life testbed. For throughput, no pattern variation relating to VWC or distance was found using the simulation. The reason might be the limited dimension topology and the low data rate. Looking at the packet reception rate, in the simulation experiment, the result showed 98% to 100% packet reception whereas the testbed had a packet reception rate of 100%.

VI. Conclusions and Future Work

In this paper, we derived an underground infrastructure-based channel model, MAME, to capture communication properties, e.g., RSSI, using WiFi and LoRaWAN. The MAME model was integrated into the NS3 simulator to understand the network behavior (RSSI and throughput) for scaled-up networks. One challenge was the absence of any existing data set for infrastructure wireless deployment. Developing such a model requires significant domain expert knowledge to encompass the physics-based attributes (e.g., reflection at interfaces, in-material absorptions, and other factors) and engineering aspects (such as concrete thickness and materials). Future work involves improving the MAME model with bigger datasets from real-life deployments, considering multi-path signal propagation, and multi-layer structures.

Acknowledgements

The authors are thankful for the support provided by Jian Peng at Orange County Public Works. This research was supported by NSF Grant No. 1952247. Any opinions, findings, and conclusions or recommendations expressed in this material are those of the authors and do not necessarily reflect the views of the National Science Foundation.

References

[1] A. B. Noel *et al.*, "Structural health monitoring using wireless sensor networks: A comprehensive survey," *IEEE Commun. Surv. Tutor.*, vol. 19, no. 3, 2017.

[2] A. E. Barbosa *et al.*, "Key issues for sustainable urban stormwater management," *Water research*, vol. 46, no. 20, pp. 6787–6798, 2012.

[3] B. Bernstein *et al.*, "Assessing urban runoff program progress through a dry weather hybrid reconnaissance monitoring design," *Environmental monitoring and assessment*, vol. 157, no. 1, pp. 287–304, 2009.

[4] R. W. Smith, "The use of random-model tolerance intervals in environmental monitoring and regulation," *JABES*, vol. 7, pp. 74–94, 2002.

[5] H. Yiğitler *et al.*, "Overview of time synchronization for iot deployments: Clock discipline algorithms and protocols," *Sensors*, vol. 20, no. 20, 2020.

[6] D. Wohwe Sambo and A. Förster, "Wireless underground sensor networks: A comprehensive survey and tutorial," *ACM Computing Surveys*, vol. 56, no. 4, October 2023.

[7] S. Islam *et al.*, "Framework for collecting data from specialized iot devices-an application to enhance healthcare systems," in *ICDH*. IEEE, 2021.

[8] A. Ayadi *et al.*, "A framework of monitoring water pipeline techniques based on sensors technologies," *JKSUCI*, vol. 34, no. 2, 2022.

[9] N. Saeed *et al.*, "Toward the internet of underground things: A systematic survey," *IEEE Commun. Surv. Tutor.*, vol. 21, no. 4, 2019.

[10] A. R. Silva and M. C. Vuran, "Empirical evaluation of wireless underground-to-underground communication in wireless underground sensor networks," in *DCOSS*. Springer, 2009.

[11] S. Mekid *et al.*, "Channel modeling and testing of wireless transmission for underground in-pipe leak and material loss detection," *IJDSN*, vol. 13, no. 11, 2017.

[12] A. R. Silva and M. C. Vuran, "Communication with aboveground devices in wireless underground sensor networks: An empirical study," in *2010 IEEE international conference on communications*. IEEE, 2010.

[13] L. Li *et al.*, "Characteristics of underground channel for wireless underground sensor networks," in *Proc. Med-Hoc-Net*, vol. 7, 2007.

[14] A. Singh *et al.*, "IoT based information and communication system for enhancing underground mines safety and productivity: Genesis, taxonomy and open issues," *Ad Hoc Networks*, vol. 78, 2018.

[15] L.-H. S. *et al.*, "Analysis and implementation for traffic-aware channel assignment and contention scheme in LoRa-based IoT networks," *IEEE Internet of Things Journal*, vol. 8, no. 14, July 2021.

[16] L. Moiroux-Arvis *et al.*, "Evaluation of LoRa technology in 433-MHz and 868-MHz for underground to aboveground data transmission," *Computers and Electronics in Agriculture*, vol. 194, 2022.

[17] "CM-Prod-Catalog," 2023. [Online]. Available: https://www.countymaterials.com/en/downloads/product-catalogs/pipe-precast/47-concrete-pipe-a-precast-product-catalog-wisconsin/file

[18] "LADPW-Manual," 2008. [Online]. Available: https://bit.ly/3w6Mwf9

[19] "Florida-DOT," 2007. [Online]. Available: https://www.fdot.gov/docs/default-source/roadway/ds/06/Int/E/205.pdf

[20] C. A. Balanis, *Antenna theory: analysis and design*. John wiley & sons, 2016.

[21] K. Siwiak, *Radiowave propagation and antennas for personal communications*. Artech House, Inc., 1998.

[22] H. Tataria *et al.*, "Standardization of propagation models for terrestrial cellular systems: A historical perspective," *Int. J. Wirel. Inf. Netw.*, vol. 28, 2021.

[23] W. E. Patitz *et al.*, "Measurement of dielectric and magnetic properties of soil," Sandia National Labs., Tech. Rep., 1995.

[24] N. R. Peplinski *et al.*, "Dielectric properties of soils in the 0.3-1.3-ghz range," *TGRS*, vol. 33, no. 3, 1995.

[25] J. Liu *et al.*, "The influence of organic matter on soil dielectric constant at microwave frequencies (0.5–40 ghz)," in *IGARSS*. IEEE, 2013.

[26] R. L. Jesch, "Dielectric measurements of five different soil textural types as functions of frequency and moisture content," *NIST*, 1978.

[27] J. Davis *et al.*, "Determination of dielectric properties of insitu concrete at radar frequencies," *NDT-CE*, 2003.

[28] S. D. Nair and R. D. Ferron, "Set-on-demand concrete," *Cement and Concrete Research*, vol. 57, 2014.

[29] F. Presuel-Moreno and A. Sagüés, "Bulk magnetic susceptibility measurements for determination of fly ash presence in concrete," *Cement and Concrete Research*, vol. 39, no. 2, 2009.

[30] M. Mukhlisin *et al.*, "Performance evaluation of volumetric water content and relative permittivity models," *The Scientific World Journal*, vol. 2013, 2013.